2

Vector sensor array processing for polarized sources using a quadrilinear representation of the data covariance

Sebastian Miron[*], Xijing Guo[*,†] and David Brie[*]
[*]*Centre de Recherche en Automatique de Nancy, Nancy-Université, CNRS France*
[†] *Department of Information and Communication Engineering, Xi'an Jiaotong University China*

1. Introduction

Array processing techniques aim principally at estimating source Directions Of Arrivals (DOA's) based on the observations recorded on a sensor array. The *vector-sensor* technology allows the use of polarization as an additional parameter, leading to *vector sensor array processing*. In electromagnetics, a vector sensor is composed of six spatially collocated but orthogonally polarized antennas, measuring all six components (three for the electric and three for the magnetic fields) of the incident wave. The benefits of considering source polarization in signal estimation were illustrated in Burgess and Van Veen (1994); Le Bihan et al. (2007); Li (1993); Miron et al. (2006); Nehorai and Paldi (1994); Rahamim et al. (2003); Weiss and Friedlander (1993a); Wong and Zoltowski (1997) for diverse signal processing problems. Most of these algorithms are based on *bilinear* polarized source mixture models which suffers from identifiability problems. This means that, without any additional constraint, the steering vectors of the sources (and implicitly their DOA's) cannot be uniquely determined by matrix factorization. The identifiability issues involved in vector sensor applications are investigated in Ho et al. (1995); Hochwald and Nehorai (1996); Tan et al. (1996a;b).

The use of polarization as a third diversity, in addition to the temporal and spatial diversities, in vector sensor array processing, leading to a trilinear mixture model, was proposed for the first time in Miron et al. (2005). Based on this model, a PARAFAC-based algorithm for signal detection, was later introduced in Zhang and Xu (2007). Multilinear models gave rise to a great interest in the signal processing community as they exhibit interesting identifiability properties; their factorization is unique under mild conditions. Several multilinear algorithms were proposed, mainly in telecommunication domain, using different diversity schemes such as code diversity Sidiropoulos et al. (2000a), multi-array diversity Sidiropoulos et al. (2000b) or time-block diversity Rong et al. (2005). For the trilinear mixture model with polarization diversity, we derived in Guo et al. (2008) the identifiability conditions and showed that in terms of source separation, the performance of the proposed algorithm is similar to the classical non-blind techniques.

Nevertheless, the joint estimation of all the three parameters of the sources (DOA, polarization, and temporal sequence) is time-consuming, and it does not always have a practical interest, especially in array processing applications. A novel stochastic algorithm for DOA estimation of polarized sources is introduced in this chapter, allowing the estimation of only two source parameters (DOA and polarization), and thus presenting a smaller computational complexity than its trilinear version Guo et al. (2008). It is based on a quadrilinear (fourth-order tensor) representation of the polarized data covariance. The parameters are then obtained by CANDECOMP/PARAFAC (CP) decomposition the covariance tensor of the polarized data, using a quadrilinear alternating least squares (QALS) approach. A significant advantage of the proposed algorithm lies in the fact that the methods based on statistical properties of the signals proved to outperform deterministic techniques Swindlehurst et al. (1997), provided that the number of samples is sufficiently high. The performance of the proposed algorithm is compared in simulations to the trilinear deterministic method, MUSIC and ESPRIT for polarized sources and to the Cramér-Rao Bound.

This chapter is organized as follows. Section 2 provides some multilinear algebra notions, necessary for the presentation of the multilinear models. In Section 3 we introduce the quadrilinear model for the covariance of the polarized data and the identifiability conditions for this model are discussed in Section 4. Section 5 presents the QALS algorithm for parameter estimation; performance and computational complexity issues are also addressed. Section 6 compares in simulations the quadrilinear algorithm to its trilinear version Guo et al. (2008), to polarized versions of MUSIC Miron et al. (2005) and ESPRIT Zoltowski and Wong (2000b) and to the CRB for vector sensor array Nehorai and Paldi (1994). We summarize our findings in Section 7.

2. Multilinear algebra preliminaries

In multilinear algebra a *tensor* is a multidimensional array. More formally, an N-way or Nth-order tensor is an element of the tensor product of N vector spaces, each of which has its own coordinate system. A first-order tensor is a vector, a second-order tensor is matrix and tensors of order three or higher are called higher-order tensors. Extending matrix notations to multilinear algebra we denote by

$$\boldsymbol{\mathcal{X}} \in \mathbb{C}^{I_1 \times I_2 \times \cdots \times I_N} \tag{1}$$

a Nth-*order* tensor with complex entries. In (1), $I_1, I_2, \ldots, I_N$ are the dimensions of the N *modes* of $\boldsymbol{\mathcal{X}}$. The entry $(i_1, i_2, \ldots, i_N)$ of $\boldsymbol{\mathcal{X}}$ is denoted by $x_{i_1 i_2 \ldots i_N}$ or by $(\boldsymbol{\mathcal{X}})_{i_1 i_2 \ldots i_N}$. For an overview of higher-order tensor their applications, the reader is referred to De Lathauwer (1997); Kolda and Bader (2007). In this section we restrain ourselves to some basic definitions and elementary operations on tensors, necessary for the understanding of the multilinear models and algorithms presented in the paper.

Definition 1 (Norm of a tensor). *The norm of a tensor $\boldsymbol{\mathcal{X}} \in \mathbb{C}^{I_1 \times I_2 \times \cdots \times I_N}$ is the square root of the sum of the squares of all its elements*, i.e.,

$$\|\boldsymbol{\mathcal{X}}\| \triangleq \sqrt{\sum_{i_1}^{I_1} \sum_{i_2}^{I_2} \cdots \sum_{i_N}^{I_N} |x_{i_1 i_2 \ldots i_N}|^2}. \tag{2}$$

This is analogous to the matrix Frobenius norm.

Definition 2 (Outer product). *The outer product of two tensors* $\mathcal{X} \in \mathbb{C}^{I_1 \times I_2 \times \cdots \times I_N}$ *and* $\mathcal{Y} \in \mathbb{C}^{J_1 \times J_2 \times \cdots \times J_P}$ *is a tensor* $\mathcal{X} \circ \mathcal{Y} \in \mathbb{C}^{I_1 \times \cdots \times I_N \times J_1 \times \cdots \times J_P}$ *defined by* $(\mathcal{X} \circ \mathcal{Y})_{i_1 \dots i_N j_1 \dots j_p} \stackrel{\triangle}{=} x_{i_1 \dots i_N} y_{j_1 \dots j_P}$.

The outer product allows to extend the rank-one matrix definition to tensors.

Definition 3 (Rank-one tensor). *An N-way tensor* $\mathcal{X} \in \mathbb{C}^{I_1 \times I_2 \times \cdots \times I_N}$ *is rank-one if it can be written as the outer product of N vectors, i.e.,*

$$\mathcal{X} = \mathbf{a}_1 \circ \mathbf{a}_2 \circ \cdots \circ \mathbf{a}_N \tag{3}$$

with $\mathbf{a}_n \in \mathbb{C}^{I_n}$.

Tensors can be multiplied together though the notation is much more complex than for matrices. Here we consider only the multiplication of a tensor by a matrix (or a vector) in mode n.

Definition 4 (n-mode product). *The n-mode product of a tensor* $\mathcal{X} \in \mathbb{C}^{I_1 \times \cdots \times I_n \times \cdots \times I_N}$ *with a matrix* $\mathbf{U} \in \mathbb{C}^{J \times I_n}$ *is denoted by* $\mathcal{X} \times_n \mathbf{U}$ *and is of size* $I_1 \times \cdots \times I_{n-1} \times J \times I_{n+1} \times \cdots \times I_N$. *It is defined as :*

$$(\mathcal{X} \times_n \mathbf{U})_{i_1 \dots i_{n-1} j i_{n+1} \dots i_N} = \sum_{i_n=1}^{I_n} x_{i_1 i_2 \dots i_N} u_{j i_n}. \tag{4}$$

Several matrix products are important in multilinear algebra formalism, two of which being recalled here.

Definition 5 (Kronecker product). *The Kronecker product of matrices* $\mathbf{A} \in \mathbb{C}^{I \times J}$ *and* $\mathbf{B} \in \mathbb{C}^{K \times L}$, *denoted by* $\mathbf{A} \otimes \mathbf{B}$, *is a matrix of size* $IK \times JL$ *defined by*

$$\mathbf{A} \otimes \mathbf{B} = \begin{bmatrix} a_{11}\mathbf{B} & \dots & a_{1J}\mathbf{B} \\ \vdots & \ddots & \vdots \\ a_{I1}\mathbf{B} & \dots & a_{IJ}\mathbf{B} \end{bmatrix} \tag{5}$$

Definition 6 (Khatri-Rao product). *Given matrices* $\mathbf{A} \in \mathbb{C}^{I \times K}$ *and* $\mathbf{B} \in \mathbb{C}^{J \times K}$, *their Khatri-Rao product is a* $IJ \times K$ *matrix defined by*

$$\mathbf{A} \odot \mathbf{B} = [\mathbf{a}_1 \otimes \mathbf{b}_1 \quad \mathbf{a}_2 \otimes \mathbf{b}_2 \quad \dots \quad \mathbf{a}_K \otimes \mathbf{b}_K], \tag{6}$$

where $\mathbf{a}_k$ *and* $\mathbf{b}_k$ *are the the columns of* $\mathbf{A}$ *and* $\mathbf{B}$, *respectively.*

A tensor can be also represented into a matrix form, process known as *matricization* or *unfolding*.

Definition 7 (Matricization). *The n-mode matricization of a tensor* $\mathcal{X} \in \mathbb{C}^{I_1 \times \cdots \times I_n \times \cdots \times I_N}$ *is a* $I_n \times I_1 \dots I_{n-1}\ I_{n+1} \dots I_N$ *size matrix denoted by* $\mathbf{X}_{(n)}$. *The tensor element* $(i_1, i_2, \dots, i_N)$ *maps to matrix element* (i_n, j) *where*

$$j = 1 + \sum_{k=1, k \neq n}^{N} (i_k - 1) J_k \quad \textit{with} \quad J_k = \prod_{m=1, m \neq n}^{k-1} I_m \tag{7}$$

This operation is generally used in the alternating least squares algorithms for fitting the CP models, as illustrated in section 5.1.

3. The quadrilinear model of the data covariance

We introduce in this section a quadrilinear model for electromagnetic source covariance, recorded on a six-component vector sensor array. Suppose the sources are completely polarized and the propagation takes place in an isotropic, homogeneous medium. We start by modeling the data measurements under the narrowband assumptions.
Consider an uniform array of M identical sensors spaced by Δx along the x-axis, collecting narrowband signals emitted from K (known *a priori*) spatially distinct far-field sources. For the kth incoming wave, its DOA can be totally determined by the azimuth angle $\phi_k \in [0, \pi)$ (measured from $+x$-axis) and the elevation angle $\psi_k \in [-\pi/2, \pi/2]$ (measured from the ground)[1], as shown in Fig. 1.

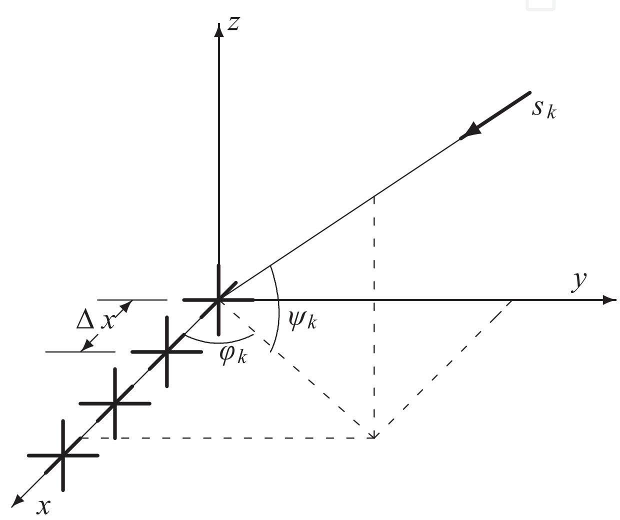

Fig. 1. 2D-DOA on a vector-sensor array

On an electromagnetic vector sensor, if the incoming wave has unit power, the electric- and magnetic-field measurements in Cartesian coordinates, $\mathbf{e}(\phi_k, \psi_k, \alpha_k, \beta_k) \triangleq [e_x^{(k)}, e_y^{(k)}, e_z^{(k)}]^T$ and $\mathbf{h}(\phi_k, \psi_k, \alpha_k, \beta_k) \triangleq [h_x^{(k)}, h_y^{(k)}, h_z^{(k)}]^T$, can be stacked up in a 6×1 vector $\mathbf{b}_k$ Nehorai and Paldi (1994)

$$\mathbf{b}_k \triangleq \begin{bmatrix} \mathbf{e}(\phi_k, \psi_k, \alpha_k, \beta_k) \\ \mathbf{h}(\phi_k, \psi_k, \alpha_k, \beta_k) \end{bmatrix} = \underbrace{\begin{bmatrix} -\sin\phi_k & -\cos\phi_k \sin\psi_k \\ \cos\phi_k & -\sin\phi_k \sin\psi_k \\ 0 & \cos\psi_k \\ -\cos\phi_k \sin\psi_k & \sin\phi_k \\ -\sin\phi_k \sin\psi_k & -\cos\phi_k \\ \cos\psi_k & 0 \end{bmatrix}}_{\mathbf{F}(\phi_k, \psi_k)} \mathbf{g}_k. \quad (8)$$

The 6×2 matrix $\mathbf{F}_k \triangleq \mathbf{F}(\phi_k, \psi_k)$ is referred to as the steering matrix Nehorai et al. (1999) and characterizes the capacity of a vector sensor to convert the information carried on an impinging polarized plane wave defined in polar coordinates, into the six electromagnetic-field-associated electric signals in the corresponding Cartesian coordinates. A 2×1 complex

[1] We assume the sources are all coming from the $+y$ side of the $x - z$ plane.

vector

$$\mathbf{g}_k \triangleq \mathbf{g}(\alpha_k, \beta_k) = \begin{bmatrix} g_\phi(\alpha_k, \beta_k) \\ g_\psi(\alpha_k, \beta_k) \end{bmatrix} = \begin{bmatrix} \cos\alpha_k & \sin\alpha_k \\ -\sin\alpha_k & \cos\alpha_k \end{bmatrix} \begin{bmatrix} \cos\beta_k \\ j\sin\beta_k \end{bmatrix} \tag{9}$$

is used to depict the polarization state of the kth signal in terms of the orientation angle $\alpha_k \in (-\pi/2, \pi/2]$ and the ellipticity angle $\beta_k \in [-\pi/4, \pi/4]$ Deschamps (1951). Now we have a compact expression $\mathbf{b}_k = \mathbf{F}(\phi_k, \psi_k)\mathbf{g}(\alpha_k, \beta_k)$ modeling the vector sensor response to the kth polarized source.

Under the far-field assumption, the spatial response of a M-sensor uniform linear array to the kth impinging wave, *i.e.* the steering vector, presents a Vandermonde structure that can be expressed as

$$\mathbf{a}_k \triangleq \mathbf{a}(\phi_k, \psi_k) = [1,\ a_k,\ \cdots,\ a_k^{M-1}]^T, \tag{10}$$

where $a_k = \exp(jk_0\Delta x \cos\phi_k \cos\psi_k)$ is the inter-sensor phase shift and k_0 is the wave number of the electromagnetic wave.

Let p $(p = 1, 2, \cdots, 6)$ index the six field components of the vector $\boldsymbol{b}_k$ respectively. Define

$$\mathbf{A} \triangleq [\mathbf{a}_1, \ldots, \mathbf{a}_K] = \begin{bmatrix} 1 & \cdots & 1 \\ a_1 & \cdots & a_k \\ \vdots & & \vdots \\ a_1^{M-1} & \cdots & a_K^{M-1} \end{bmatrix} \tag{11}$$

a $M \times K$ matrix containing the spatial responses of the array to the N sources,

$$\mathbf{B} \triangleq [\mathbf{b}_1, \ldots, \mathbf{b}_K] = [\mathbf{F}_1\mathbf{g}_1, \ldots, \mathbf{F}_K\mathbf{g}_K] \tag{12}$$

a $6 \times K$ matrix containing the polarization responses and

$$\mathbf{S} \triangleq \begin{bmatrix} s_1 & \cdots & 0 \\ \vdots & \ddots & \vdots \\ 0 & \cdots & s_K \end{bmatrix} \tag{13}$$

a $K \times K$ diagonal matrix containing the K source signals at some fixed instant. With these notations, a snapshot of the output of the array can be organized as a $M \times 6$ matrix

$$\mathbf{X} = \mathbf{A}\mathbf{S}\mathbf{B}^T + \mathbf{N} \tag{14}$$

with $\mathbf{N}$ a $M \times 6$ matrix expressing the noise contribution on the antenna.

The following assumptions are made

(A1) Sources are zero-mean, stationary, mutually uncorrelated, ergodic processes

(A2) The noise is i.i.d. centered, complex Gaussian process of variance σ^2, non-polarized and spatially white

(A3) The sources have distinct DOAs

We define the 4-way covariance of the received data as the $M \times 6 \times M \times 6$ array

$$\mathcal{C}_{XX} \triangleq \mathrm{E}\{\mathbf{X} \circ \mathbf{X}^*\} \tag{15}$$

where $\mathrm{E}\{.\}$ denotes the mathematical expectation operation. We define also the source covariance as the $K \times K \times K \times K$ fourth-order tensor

$$\mathcal{C}_{SS} \stackrel{\triangle}{=} \mathrm{E}\{\mathbf{S} \circ \mathbf{S}^*\} \tag{16}$$

From (14) and (16) and using assumptions (A1) and (A2) the covariance tensor of the received data takes the following form

$$\mathcal{C}_{XX} = \mathcal{C}_{SS} \times_1 \mathbf{A} \times_2 \mathbf{B} \times_3 \mathbf{A}^* \times_4 \mathbf{B}^* + \mathcal{N} \tag{17}$$

where $\mathcal{N}$ is a $M \times 6 \times M \times 6$ tensor containing the noise power on the sensors. Assumption (A1) implies that $\mathcal{C}_{SS}$ is a hyperdiagonal tensor (the only non-null entries are those having all four indices identical), meaning that $\mathcal{C}_{XX}$ presents a *quadrilinear* CP structure Harshman (1970). The inverse problem for the direct model expressed by (17) is the estimation of matrices **A** and **B** starting from the 4-way covariance tensor $\mathcal{C}_{XX}$.

4. Identifiability of the quadrilinear model

Before addressing the problem of estimating **A** and **B**, the identifiability of the quadrilinear model (17) must be studied first. The polarized mixture model (17) is said to be *identifiable* if **A** and **B** can be uniquely determined (up to permutation and scaling indeterminacies) from $\mathcal{C}_{XX}$. In multilinear framework Kruskal's condition is a sufficient condition for unique CP decomposition, relying on the concept of Kruskal-rank or (k-rank) Kruskal (1977).

Definition 8 (k-rank)**.** *Given a matrix $\mathbf{A} \in \mathbb{C}^{I \times J}$, if every linear combination of l columns has full column rank, but this condition does not hold for $l+1$, then the k-rank of **A** is l, written as $k_{\mathbf{A}} = l$.*

Note that $k_{\mathbf{A}} \leq \mathrm{rank}(\mathbf{A}) \leq \min(I, J)$, and both equalities hold when $\mathrm{rank}(\mathbf{A}) = J$.
Kruskal's condition was first introduced in Kruskal (1977) for the three-way arrays and generalized later on to multi-way arrays in Sidiropoulos and Bro (2000). We formulate next Kruskal's condition for the quadrilinear mixture model expressed by (17), considering the noiseless case ($\mathcal{N}$ in (17) has only zero entries).

Theorem 1 (Kruskal's condition)**.** *Consider the four-way CP model (17). The loading matrices **A** and **B** can be uniquely estimated (up to column permutation and scaling ambiguities), if but not necessarily*

$$k_{\mathbf{A}} + k_{\mathbf{B}} + k_{\mathbf{A}^*} + k_{\mathbf{B}^*} \geq 2K + 3 \tag{18}$$

This implies

$$k_{\mathbf{A}} + k_{\mathbf{B}} \geq K + 2 \tag{19}$$

It was proved Tan et al. (1996a) that in the case of vector sensor arrays, the responses of a vector sensor to every three sources of distinct DOA's are linearly independent regardless of their polarization states. This means, under the assumption (A3) that $k_{\mathbf{B}} \geq 3$. Furthermore, as **A** is a Vandermonde matrix, (A3) also guarantees that $k_{\mathbf{A}} = \min(M, K)$. All these results sum up into the following corollary:

Corollary 1. *Under the assumptions (A1)-(A3), the DOA's of K uncorrelated sources can be uniquely determined using an M-element vector sensor array if $M \geq K - 1$, regardless of the polarization states of the incident signals.*

This sufficient condition also sets an upper bound on the minimum number of sensors needed to ensure the identifiability of the polarized mixture model. However, the condition $M \geq K - 1$ is not necessary when considering the polarization states, that is, a lower number of sensors can be used to identify the mixture model, provided that the polarizations of the sources are different. Also the symmetry properties of $\boldsymbol{\mathcal{C}}_{XX}$ are not considered and we believe that they can be used to obtain milder sufficient conditions for ensuring the identifiability.

5. Source parameters estimation

We present next the algorithm used for estimating sources DOA's starting from the observations on the array and address some issues regarding the accuracy and the complexity of the proposed method.

5.1 Algorithm

Supposing that L snapshots of the array are recorded and using (A1) an estimate of the polarized data covariance (15) can be obtained as the temporal sample mean

$$\hat{\boldsymbol{\mathcal{C}}}_{XX} = \frac{1}{L}\sum_{l=1}^{L} \mathbf{X}(l) \circ \mathbf{X}^*(l). \tag{20}$$

For obvious matrix conditioning reasons, the number of snapshots should be greater or equal to the number of sensors, *i.e.* $L \geq K$.

The algorithm proposed in this section includes three sequential steps, during which the DOA information is extracted and then refined to yield the final DOA's estimates. These three steps are presented next.

5.1.1 Step 1

This first step of the algorithm is the estimation of the loading matrices $\mathbf{A}$ and $\mathbf{B}$ from $\hat{\boldsymbol{\mathcal{C}}}_{XX}$. This estimation procedure can be accomplished via the *Quadrilinear Alternative Least Squares (QALS)* algorithm Bro (1998), as shown next.
Denote by $\hat{\mathbf{C}}_{pq} = \hat{\boldsymbol{\mathcal{C}}}_{XX}(:,p,:,q)$ the (p,q)th matrix slice $(M \times M)$ of the covariance tensor $\hat{\boldsymbol{\mathcal{C}}}_{XX}$. Also note $\mathrm{D}_p(\cdot)$ the operator that builds a diagonal matrix from the pth row of another and $\boldsymbol{\Delta} = \mathrm{diag}\left(E\|s_1\|^2, \ldots, E\|s_K\|^2\right)$, the diagonal matrix containing the powers of the sources. The matrices $\mathbf{A}$ and $\mathbf{B}$ can then be determined by minimizing the Least Squares (LS) criterion

$$\phi(\sigma, \boldsymbol{\Delta}, \mathbf{A}, \mathbf{B}) = \sum_{p,q=1}^{6} \left\| \hat{\mathbf{C}}_{pq} - \mathbf{A}\boldsymbol{\Delta}\mathrm{D}_p(\mathbf{B})\mathrm{D}_q(\mathbf{B}^*)\mathbf{A}^H - \sigma^2\delta_{pq}\mathbf{I}_M \right\|_F^2 \tag{21}$$

that equals

$$\begin{aligned}\phi(\sigma, \boldsymbol{\Delta}, \mathbf{A}, \mathbf{B}) = &\sum_{p,q} \left\| \hat{\mathbf{C}}_{pq} - \mathbf{A}\boldsymbol{\Delta}\mathrm{D}_p(\mathbf{B})\mathrm{D}_q(\mathbf{B}^*)\mathbf{A}^H \right\|_F^2 \\ &- 2\sigma^2 \sum_{p} \Re\left\{ \mathrm{tr}\left(\hat{\mathbf{C}}_{pp} - \mathbf{A}\boldsymbol{\Delta}\mathrm{D}_p(\mathbf{B})\mathrm{D}_p(\mathbf{B}^*)\mathbf{A}^H \right) \right\} + 6M\sigma^4\end{aligned} \tag{22}$$

where $\mathrm{tr}(\cdot)$ computes the trace of a matrix and $\Re(\cdot)$ denotes the real part of a quantity.

$$\phi(\sigma, \mathbf{\Delta}, \mathbf{A}, \mathbf{B}) = \sum_{p,q} \left\| \hat{\mathbf{C}}_{pq} - \mathbf{A}\mathbf{\Delta}\mathrm{D}_p(\mathbf{B})\mathrm{D}_q(\mathbf{B}^*)\mathbf{A}^H \right\|_F^2 - 2\sigma^2 \sum_p \Re\left\{ \mathrm{tr}\left(\hat{\mathbf{C}}_{pp} - 2M\mathbf{\Delta} \right) \right\} + 6M\sigma^4 \tag{23}$$

Thus, finding $\mathbf{A}$ and $\mathbf{B}$ is equivalent to the minimization of (23) with respect to $\mathbf{A}$ and $\mathbf{B}$, i.e.

$$\{\hat{\mathbf{A}}, \hat{\mathbf{B}}\} = \min_{\mathbf{A},\mathbf{B}} \omega(\Delta, \mathbf{A}, \mathbf{B}) \tag{24}$$

subject to $\|\boldsymbol{a}_k\|^2 = M$ and $\|\boldsymbol{b}_k\|^2 = 2$, where

$$\omega(\Delta, \mathbf{A}, \mathbf{B}) = \sum_{p,q} \left\| \hat{\mathbf{C}}_{pq} - \mathbf{A}\mathbf{\Delta}\mathrm{D}_p(\mathbf{B})\mathrm{D}_q(\mathbf{B}^*)\mathbf{A}^H \right\|_F^2 \tag{25}$$

The optimization process in (24) can be implemented using QALS algorithm, briefly summarized as follows.

Algorithm 1 QALS algorithm for four-way symmetric tensors

INPUT: the estimated data covariance $\hat{\boldsymbol{\mathcal{C}}}_{XX}$ and the number of the sources K
Initialize the loading matrices $\mathbf{A}$, $\mathbf{B}$ randomly, or using ESPRIT Zoltowski and Wong (2000a) for a faster convergence
Set $\mathbf{C} = \mathbf{A}^*$ and $\mathbf{D} = \mathbf{B}^*$.
repeat
    $\mathbf{A} = \mathbf{X}_{(1)}[(\mathbf{B} \odot \mathbf{C} \odot \mathbf{D})^\dagger]^T$
    $\mathbf{B} = \mathbf{X}_{(2)}[(\mathbf{C} \odot \mathbf{D} \odot \mathbf{A})^\dagger]^T$
    $\mathbf{C} = \mathbf{X}_{(3)}[(\mathbf{D} \odot \mathbf{A} \odot \mathbf{B})^\dagger]^T$
    $\mathbf{D} = \mathbf{X}_{(4)}[(\mathbf{A} \odot \mathbf{B} \odot \mathbf{C})^\dagger]^T$,
    where $(\cdot)^\dagger$ denotes Moore-Penrose pseudoinverse of a matrix
    Update $\mathbf{C}$, $\mathbf{D}$ by $\mathbf{C} := (\mathbf{A}^* + \mathbf{C})/2$ and $\mathbf{D} := (\mathbf{B}^* + \mathbf{D})/2$
until convergence
OUTPUT: estimates of $\mathbf{A}$ and $\mathbf{B}$.

Once the $\hat{\mathbf{A}}$, $\hat{\mathbf{B}}$ are estimated, the following post-processing is needed for the refined DOA estimation.

5.1.2 Step 2

The second step of our approach extracts separately the DOA information contained by the columns of $\hat{\mathbf{A}}$ (see eq. (10)) and $\hat{\mathbf{B}}$ (see eq. (8)).

First the estimated matrix $\hat{\mathbf{B}}$ is exploited via the physical relationships between the electric and magnetic field given by the Poynting theorem. Recall the Poynting theorem, which reveals the mutual orthogonality nature among the three physical quantities related to the kth source: the electric field $\mathbf{e}_k$, the magnetic field $\mathbf{h}_k$, and the kth source's direction of propagation, *i.e.*, the normalized Poynting vector $\mathbf{u}_k$.

$$\mathbf{u}_k = \begin{bmatrix} \cos\phi_k \cos\psi_k \\ \sin\phi_k \cos\psi_k \\ \sin\psi_k \end{bmatrix} = \Re\left(\frac{\mathbf{e}_k \times \mathbf{h}_k^*}{\|\mathbf{e}_k\| \cdot \|\mathbf{h}_k\|}\right). \tag{26}$$

Equation (26) gives the cross-product DOA estimator, as suggested in Nehorai and Paldi (1994). An estimate of the Poynting vector for the kth source $\hat{\mathbf{u}}_k$ is thus obtained, using the previously estimated $\hat{\mathbf{e}}_k$ and $\hat{\mathbf{b}}_k$.

Secondly, matrix $\hat{\mathbf{A}}$ is used to extract the DOA information embedded in the Vandermonde structure of its columns $\hat{\mathbf{a}}_k$.
Given the noisy steering vector $\hat{\mathbf{a}} = [\hat{a}_0\ \hat{a}_1\ \cdots\ \hat{a}_{M-1}]^T$, its Fourier spectrum is given by

$$A(\omega) = \frac{1}{M}\sum_{m=0}^{M-1} \hat{a}_m \exp(-jm\omega) \tag{27}$$

as a function of ω.
Given the Vandermonde structure of the steering vectors, the spectrum magnitude $|A(\omega)|$ in the absence of noise is maximum for $\omega = \omega_0$. In the presence of Gaussian noise, $\max_\omega |A(\omega)|$ provides an maximum likelihood (ML) estimator for $\omega_0 \triangleq k_0 \Delta x \cos\phi \cos\psi$ as shown in Rife and Boorstyn (1974).
In order to get a more accurate estimator of $\omega_0 \triangleq k_0 \Delta x \cos\phi \cos\psi$, we use the following processing steps.

1) We take uniformly Q ($Q \geq M$) samples from the spectrum $A(\omega)$, say $\{A(2\pi q/Q)\}_{q=0}^{Q-1}$, and find the *coarse* estimate $\hat{\omega} = 2\pi\check{q}/Q$ so that $A(2\pi\check{q}/Q)$ has the maximum magnitude. These spectrum samples are identified via the fast Fourier transform (FFT) over the zero-padded Q-element sequence $\{\hat{a}_0, \ldots, \hat{a}_{M-1}, 0, \ldots, 0\}$.
2) Initialized with this coarse estimate, the *fine* estimate of ω_0 can be sought by maximizing $|A(\omega)|$. For example, the *quasi-Newton* method (see, *e.g.*, Nocedal and Wright (2006)) can be used to find the maximizer $\hat{\omega}_0$ over the local range $\left(\frac{2\pi(\check{q}-1)}{Q}, \frac{2\pi(\check{q}+1)}{Q}\right)$.

The normalized phase-shift can then be obtained as $\varrho = (k_0\Delta x)^{-1} \arg(\hat{\omega}_0)$.

5.1.3 Step 3

In the third step, the two DOA information, obtained at **Step 2**, are combined in order to get a refined estimation of the DOA parameters ϕ and ψ. This step can be formulated as the following non-linear optimization problem

$$\min_{\psi,\phi} \left\| \begin{bmatrix} \cos\phi\cos\psi \\ \sin\phi\cos\psi \\ \sin\psi \end{bmatrix} - \hat{\mathbf{u}} \right\| \quad \text{subject to } \cos\phi\cos\psi = \varrho. \tag{28}$$

A closed form solution to (28) can be found by transforming it into an alternate problem of 3-D geometry, *i.e.* finding the point on the vertically posed circle $\cos\phi\cos\psi = \varrho$ which minimizes its Euclidean distance to the point $\hat{\mathbf{u}}$, as shown in Fig. 2.
To solve this problem, we do the orthogonal projection of $\hat{\mathbf{u}}$ onto the plane $x = \varrho$ in the 3-D space, then join the perpendicular foot with the center of the circle by a piece of line segment.

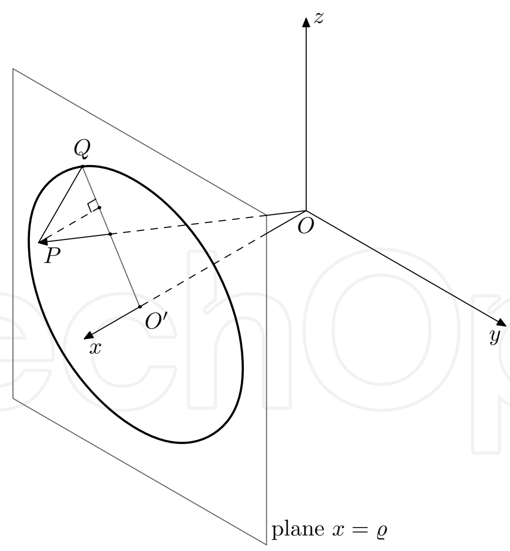

Fig. 2. Illustration of the geometrical solution to the optimization problem (28). The vector $\vec{OP}$ represents the coarse estimate of Poynting vector $\hat{\mathbf{u}}$. It is projected orthogonally onto the $x = \varrho$ plane, forming a shadow cast $\overline{O'Q}$, where O' is the center of the circle of center O on the plane given in the polar coordinates as $\cos\phi\cos\psi = \varrho$. The refined estimate, obtained this way, lies on $\overline{O'Q}$. As it is also constrained on the circle, it can be sought as their intersection point Q.

This line segment collides with the circumference of the circle, yielding an intersection point, that is the minimizer of the problem.
Let $\hat{\mathbf{u}} \triangleq [\hat{u}_1\ \hat{u}_2\ \hat{u}_3]^T$ and define $\kappa \triangleq \hat{u}_3/\hat{u}_2$, then the intersection point is given by

$$\left[\begin{array}{ccc} \varrho & \pm\sqrt{\frac{1-\varrho^2}{1+\kappa^2}} & \pm|\kappa|\sqrt{\frac{1-\varrho^2}{1+\kappa^2}} \end{array}\right]^T \tag{29}$$

where the signs are taken the same as their corresponding entries of vector $\hat{\mathbf{u}}$. Thus, the azimuth and elevation angles estimates are given by

$$\hat{\phi} = \begin{cases} \arctan \frac{1}{|\varrho|}\sqrt{\frac{1-\varrho^2}{1+\kappa^2}}, & \text{if } \varrho \geq 0 \\ \pi - \arctan \frac{1}{|\varrho|}\sqrt{\frac{1-\varrho^2}{1+\kappa^2}}, & \text{if } \varrho < 0 \end{cases} \tag{30a}$$

$$\hat{\psi} = \arcsin\sqrt{\varrho^2 + \frac{1-\varrho^2}{1+\kappa^2}}, \tag{30b}$$

which completes the DOA estimation procedure. The polarization parameters can be obtained in a similar way from $\hat{\mathbf{B}}$.
It is noteworthy that this algorithm is not necessarily limited to uniform linear arrays. It can be applied to arrays of arbitrary configuration, with minimal modifications.

5.2 Estimator accuracy and algorithm complexity issues

This subsection aims at giving some analysis elements on the accuracy and complexity of the proposed algorithm (QALS) used for the DOA estimation.

An exhaustive and rigorous performance analysis of the proposed algorithm is far from being obvious. However, using some simple arguments, we provide elements giving some insights into the understanding of the performance of the QALS and allowing to interpret the simulation results presented in section 6.

Cramér-Rao bounds were derived in Liu and Sidiropoulos (2001) for the decomposition of multi-ways arrays and in Nehorai and Paldi (1994) for vector sensor arrays. It was shown Liu and Sidiropoulos (2001) that higher dimensionality benefits in terms of CRB for a given data set. To be specific, consider a data set represented by a four-way CP model. It is obvious that, unfolding it along one dimension, it can also be represented by a three-way model. The result of Liu and Sidiropoulos (2001) states that than a quadrilinear estimator normally yields better performance than a trilinear one. In other word, the use of a four-way ALS on the covariance tensor is better sounded that performing a three-way ALS on the unfolded covariance tensor. A comparaison can be conducted with respect to the three-way CP estimator used in Guo et al. (2008), that will be denoted TALS. The addressed question is the following : is it better to perform the trilinear decomposition of the 3-way raw data tensor or the quadriliear decomposition of the 4-way convariance tensor ?
To compare the accuracy of the two algorithms we remind that the variance of an unbiased linear estimator of a set of independant parameters is of the order of $\mathcal{O}\left(\frac{\mathrm{P}}{\mathrm{N}}\sigma^2\right)$, where P is the number of parameters to estimate and N is the number of samples.
Coming back to the QALS and TALS methods, the main difference between them is that the trilinear approach estimates (in addition to $\mathbf{A}$ and $\mathbf{B}$), the K temporal sequences of size L. More precisely, the number of parameters to estimate equals $(6 + M + L)K$ for the three-way approach and $(6 + M)K$ for the quadrilinear method. Nevertheless, TALS is directly applied on the three-way raw data, meaning that the number of available observations (samples) is $6ML$ while QALS is based on the covariance of the data which, because of the symmetry of the covariance tensor, reduces the samples number to half of the entries of $\hat{\boldsymbol{\mathcal{C}}}_{XX}$, that is $18M^2$. The point is that the noise power for the covariance of the data is reduced by the averaging in (20) to σ^2/L. If we resume, the estimation variance for TALS is of the order of $\mathcal{O}\left(\frac{(6+M+L)K}{6ML}\sigma^2\right)$ and of $\mathcal{O}\left(\frac{(6+M)K}{18M^2}\frac{\sigma^2}{L}\right)$ for QALS. Let us now analyse the typical situation consisting in having a large number of time samples. For large values of L, $(L \gg (M + 6))$, the variance of TALS tends to a constant value $\mathcal{O}\left(\frac{K}{6M}\sigma^2\right)$ while for QALS it tends to 0. This means that QALS improves continuously with the sample size while this is not the case for TALS. This analysis also applies to the case of MUSIC and ESPRIT since both also work on time averaged data.

We address next some computational complexity aspects for the two previously discussed algorithms. Generally, for an N-way array of size $I_1 \times I_2 \times \cdots \times I_N$, the complexity of its CP decomposition in a sum of K rank-one tensors, using ALS algorithm is $\mathcal{O}(K\prod_{n=1}^{N} I_n)$ Rajih and Comon (2005), for each iteration. Thus, for one iteration, the number of elementary operations involved is QALS is of order $\mathcal{O}(6^2KM^2)$ and of the order of $\mathcal{O}(6KML)$ for TALS. Normally $6M \ll L$, meaning that for large data sets QALS should be much faster than its trilinear counterpart. In general, the number of iterations required for the decomposition convergence, is not determined by the data size only, but is also influenced by the initialisation and the

parameter to estimate. This makes an exact theoretical analysis of the algorithms complexity rather difficult. Moreover, trilinear factorization algorithms have been extensively studied over the last two decades, resulting in improved, fast versions of ALS such as COMFAC[2], while the algorithms for quadrilinear factorizations remained basic. This makes an objective comparison of the complexity of the two algorithms even more difficult.
Compared to MUSIC-like algorithms, which are also based on the estimation of the data covariance, the main advantage of QALS is the identifiability of the model. While MUSIC generally needs an exhaustive grid search for the estimation of the source parameters, the quadrilinear method yields directly the steering and the polarization vectors for each source.

6. Simulations and results

In this section, some typical examples are considered to illustrate the performance of the proposed algorithm with respect to different aspects. In all the simulations, we assume the inter-element spacing between two adjacent vector sensors is half-wavelength, *i.e.*, $\Delta x = \lambda/2$ and each point on the figures is obtained through $R = 500$ independent Monte Carlo runs. We divided this section into two parts. The first aims at illustrating the efficiency of the novel method for the estimation of both DOA parameters (azimuth and elevation angles) and the second shows the effects of different parameters on the method. Comparisons are conducted to recent high-resolution eigenstructure-based algorithms for polarized sources and to the CRB Nehorai and Paldi (1994).

Example 1: This example is designed to show the efficiency of the proposed algorithm using a uniform linear array of vector sensors for the 2D DOA estimation problem. It is compared to MUSIC algorithm for polarized sources, presented under different versions in Ferrara and Parks (1983); Gong et al. (2009); Miron et al. (2005); Weiss and Friedlander (1993b), to TALS Guo et al. (2008) and the Cramér-Rao bound for vector sensor arrays proposed by Nehorai Nehorai and Paldi (1994). A number of $K = 2$ equal power, uncorrelated sources are considered. The DOA's are set to be $\phi_1 = 20^\circ$, $\psi_1 = 5^\circ$ for the first source and $\phi_2 = 30^\circ$, $\psi_2 = 10^\circ$ for the other; the polarization states are $\alpha_1 = \alpha_2 = 45^\circ$, $\beta_1 = -\beta_2 = 15^\circ$. In the simulations, $M = 7$ sensors are used and in total $L = 100$ temporal snapshots are available. The performance is evaluated in terms of root-mean-square error (RMSE). In the following simulations we convert the angular RMSE from radians to degrees to make the comparisons more intuitive. The performances of these algorithms are shown in Fig. 3(a) and (b) versus the increasing signal-to-noise ratio (SNR). The SNR is defined per source and per field component ($6M$ field components in all). One can observe that all the algorithms present similar performance and eventually achieve the CRB for high SNR's (above 0 dB in this scenario). At low SNR's, nonetheless, our algorithm outperforms MUSIC, presenting a lower SNR threshold (about 8 dB) for a meaningful estimate. CP methods (TALS and QALS), which are based on the LS criterion, are demonstrated to be less sensitive to the noise than MUSIC. This confirms the results presented in Liu and Sidiropoulos (2001) that higher dimension (an increased structure of the data) benefits in terms of estimation accuracy.
Example 2: We examine next the performance of QALS in the presence of four uncorrelated sources. For simplicity, we assume all the elevation angles are zero, $\psi_k = 0^\circ$ for $k = 1, \ldots, 4$, and some typical values are chosen for the azimuth angles, respectively: $\phi_1 = 10^\circ$, $\phi_2 = 20^\circ$,

[2] COMFAC is a fast implementation of trilinear ALS working with a compressed version of the data Sidiropoulos et al. (2000a)

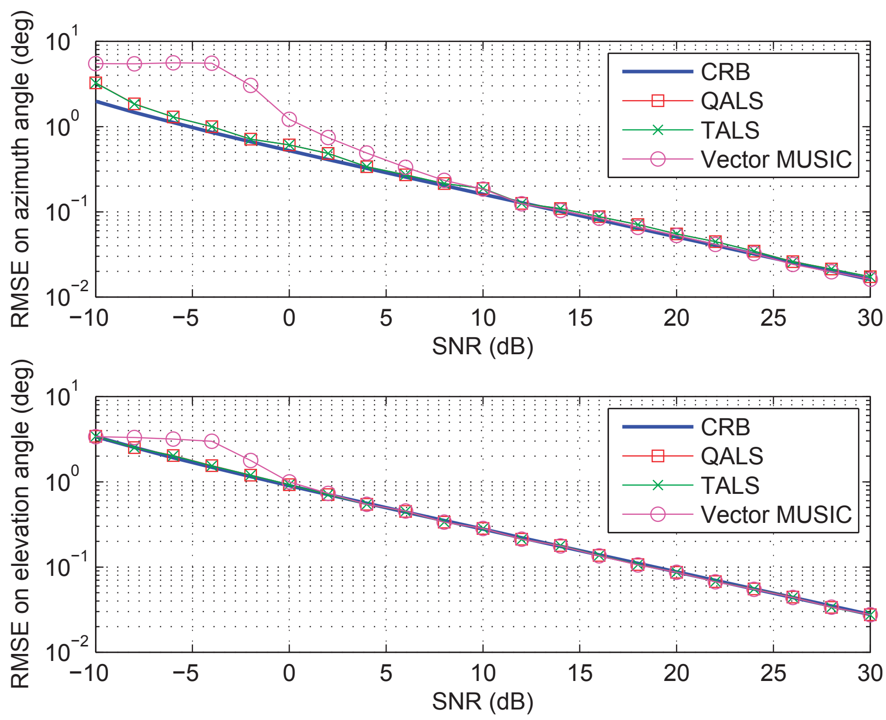

(a) RMSE of the DOA estimation for the first source

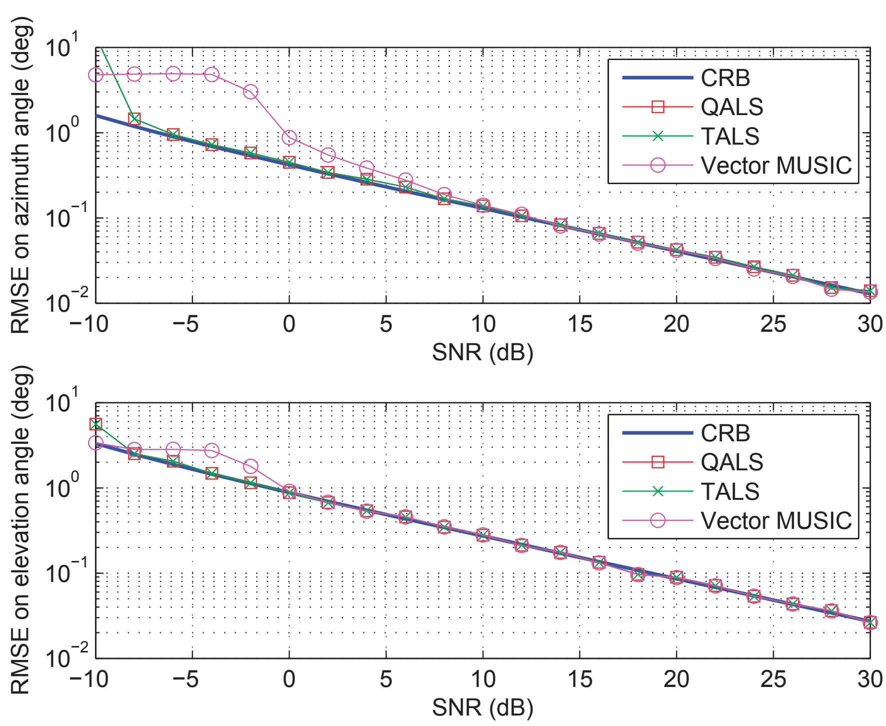

(b) RMSE of the DOA estimation for the second source

Fig. 3. RMSE of the DOA estimation versus SNR in the presence of two uncorrelated sources

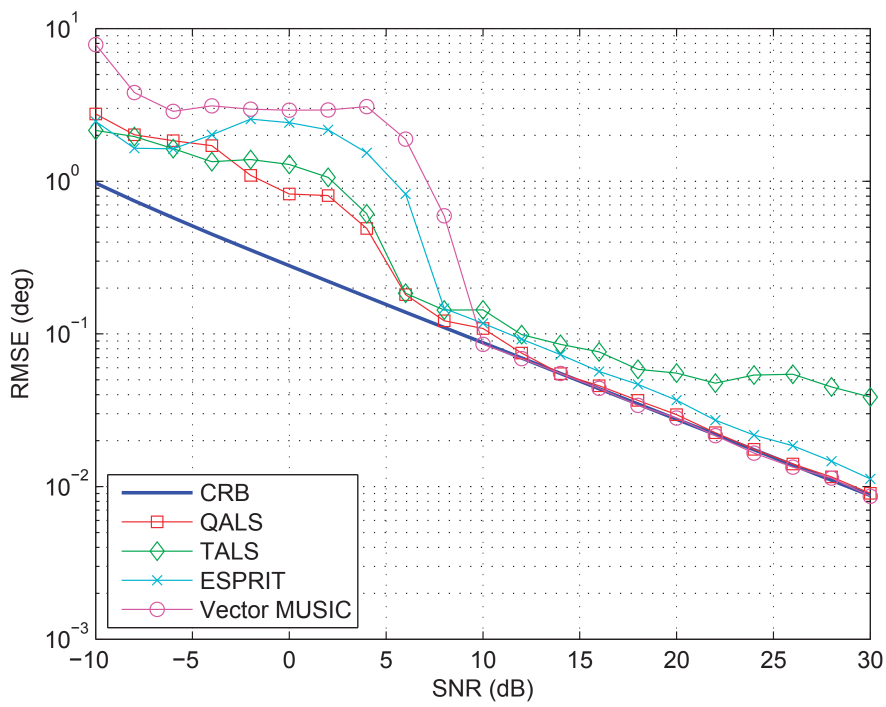

Fig. 4. RMSE of azimuth angle estimation versus SNR for the second source in the presence of four uncorrelated sources

$\phi_1 = 30°$, $\phi_1 = 40°$. The polarizations parameters are $\alpha_2 = -45°$, $\beta_2 = -15°$ for the second source and for the others, the sources have equal orientation and ellipticity angles, 45° and 15° respectively. We keep the same configuration of the vector sensor array as in example 1. For this example we compare our algorithm to polarized ESPRIT Zoltowski and Wong (2000a;b) as well. The following three sets of simulations are designed with respect to the increasing value of SNR, number of vector sensors and snapshots.

Fig. 4 shows the comparison between the four algorithms as the SNR increases. Once again, the advantage of the multilinear approaches in tackling DOA problem at low SNR's can be observed. The quadrilinear approach seems to perform better than TALS as the SNR increases. The MUSIC algorithm is more sensitive to the noise than all the others, yet it reaches the CRB as the SNR is high enough. The estimate obtained by ESPRIT is mildly biased.

Next, we show the effect of the number of vector sensors on the estimators. The SNR is fixed to 20 dB and all the other simulation settings are preserved. The results are illustrated on Fig. 5. One can see that the DOA's of the four sources can be uniquely identified with only two vector sensors (RMSE around 1°), which substantiates our statement on the identifiablity of the model in Section 4. As expected, the estimation accuracy is reduced by decreasing the number of vector sensors, and the loss becomes important when only few sensors are present (four sensors in this case). Again ESPRIT yieds biased estimates. For the trilinear method, it is shown that its performance limitation, observed on Fig. 4, can be tackled by using more sensors, meaning that the array aperture is a key parameter for TALS. The MUSIC method shows mild advantages over the quadrilinear one in the case of few sensors (less than four sensors), yet the two yield comparable performance as the number of vector sensors increases (superior to the other two methods).

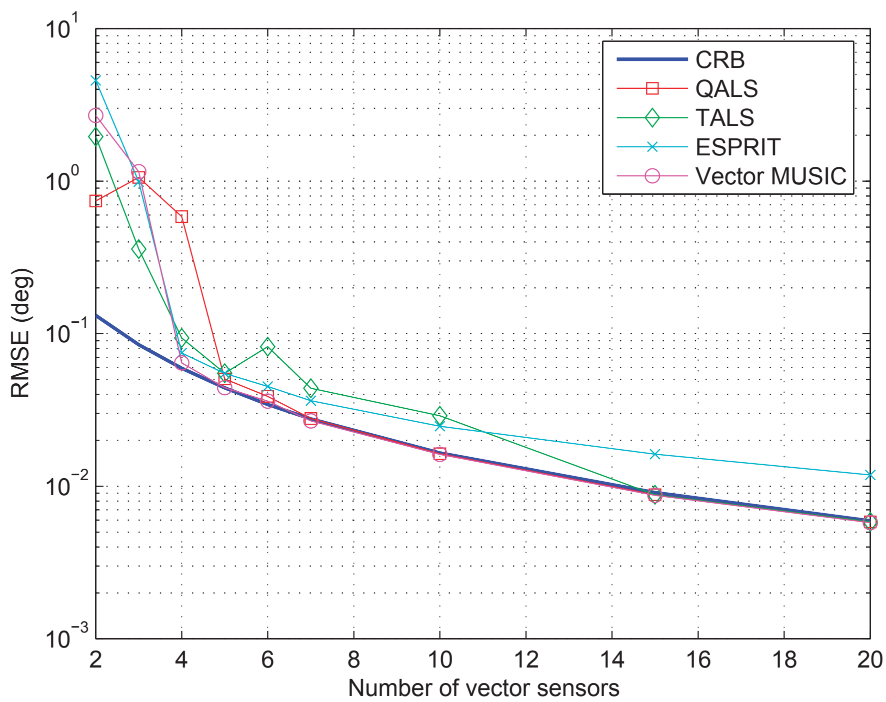

Fig. 5. RMSE of azimuth angle estimation versus the number of vector sensors for the second source in the presence of four uncorrelated sources

Finally, we fix the SNR at 20 dB, while keeping the other experimental settings the same as in Fig. 4, except for an increasing number of snapshots L which varies from 10 to 1000. Fig. 6 shows the varying RMSE with respect to the number of snapshots in estimating azimuth angle of the second source. Once again, the proposed algorithm performs better than TALS. Moreover as L becomes important, one can see that TALS tends to a constant value while the RMSE for QALS continues to decrease, which confirms the theoretical deductions presented in subsection 5.2.

7. Conclusions

In this paper we introduced a novel algorithm for DOA estimation for polarized sources, based on a four-way PARAFAC representation of the data covariance. A quadrilinear alternated least squares procedure is used to estimate the steering vectors and the polarization vectors of the sources. Compared to MUSIC for polarized sources, the proposed algorithm ensures the mixture model identifiability; thus it avoids the exhaustive grid search over the parameters space, typical to eigestructure algorithms. An upper bound on the minimum number of sensors needed to ensure the identifiability of the mixture model is derived. Given the symmetric structure of the data covariance, our algorithm presents a smaller complexity per iteration compared to three-way PARAFAC applied directly on the raw data. In terms of estimation, the proposed algorithm presents slightly better performance than MUSIC and ESPRIT, thanks to its higher dimensionality and it clearly outperforms the three-way algorithm when the number of temporal samples becomes important. The variance of our algorithm decreases with an increase in the sample size while for the three-way method it tends asymptotically to a constant value.

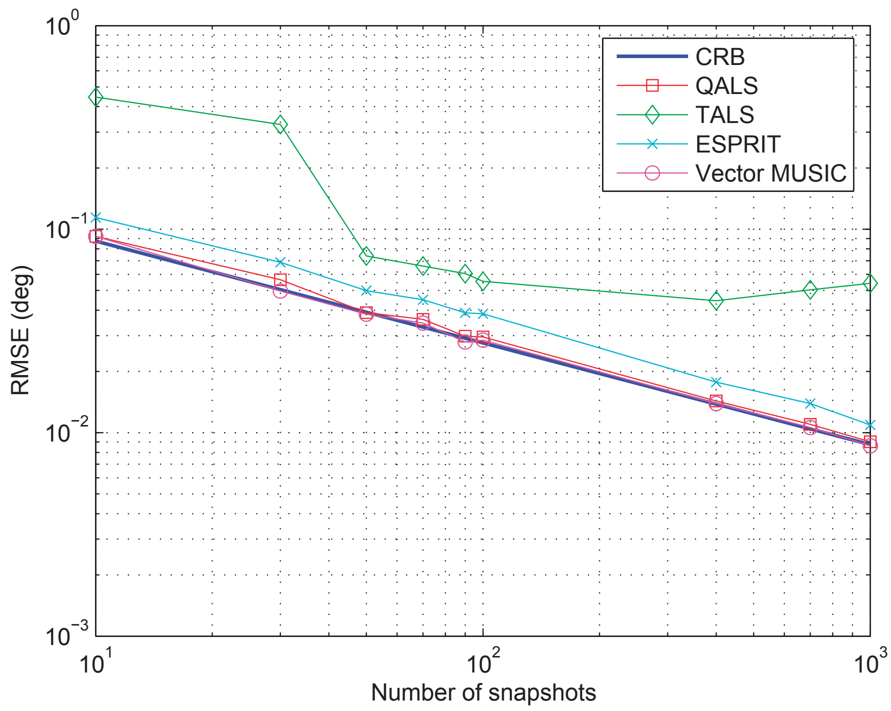

Fig. 6. RMSE of azimuth angle estimation versus the number of snapshots for the second source in the presence of four uncorrelated sources

Future works should focus on developing faster algorithms for four-way PARAFAC factorization in order to take full advantage of the lower complexity of the algorithm. Also, the symmetry of the covariance tensor must be taken into account to derive lower bounds on the minimum number of sensors needed to ensure the source mixture identifiability.

8. References

Bro, R. (1998). Multi-way Analysis in the Food Industry - Models, Algorithms, and Applications. Ph.D. dissertation. Royal Veterinary and Agricultural University. Denmark.

Burgess, K. A. and B. D. Van Veen (1994). A subspace GLRT for vector-sensor array detection. In: *Proc. IEEE Int. Conf. Acoust., Speech, Signal Process. (ICASSP)*. Vol. 4. Adelaide, SA, Australia. pp. 253–256.

De Lathauwer, L. (1997). Signal Processing based on Multilinear Algebra. PhD thesis. Katholieke Universiteit Leuven.

Deschamps, G. A. (1951). Geometrical representation of the polarization of a plane electromagnetic wave. *Proc. IRE* **39**, 540–544.

Ferrara, E. R., Jr. and T. M. Parks (1983). Direction finding with an array of antennas having diverse polarizations. *IEEE Trans. Antennas Propagat.* **AP-31**(2), 231–236.

Gong, X., Z. Liu, Y. Xu and M. I. Ahmad (2009). Direction-of-arrival estimation via twofold mode-projection. *Signal Processing* **89**(5), 831–842.

Guo, X., S. Miron and D. Brie (2008). Identifiability of the PARAFAC model for polarized source mixture on a vector sensor array. In: *Proc. IEEE ICASSP 2008*. Las Vegas, USA.

Harshman, R. A. (1970). Foundations of the PARAFAC procedure: Model and conditions for an explanatory multi-mode factor analysis. *UCLA Working Papers Phonetics*, **16**, 1–84.

Ho, K.-C., K.-C. Tan and W. Ser (1995). An investigation on number of signals whose directions-of-arrival are uniquely determinable with an electromagnetic vector sensor. *Signal Process.* **47**(1), 41–54.

Hochwald, B. and A. Nehorai (1996). Identifiability in array processing models with vector-sensor applications. *IEEE Trans. Signal Process.* **44**(1), 83–95.

Kolda, T. G. and B. W. Bader (2007). Tensor decompositions and applications. Technical Report SAND2007-6702. Sandia National Laboratories. Albuquerque, N. M. and Livermore.

Kruskal, J. B. (1977). Three-way arrays: Rank and uniqueness of trilinear decompositions, with application to arithmetic complexity and statistics. *Linear Algebra Applicat.* **18**, 95–138.

Le Bihan, N., S. Miron and J. I. Mars (2007). MUSIC algorithm for vector-sensors array using biquaternions. *IEEE Trans. Signal Process.* **55**(9), 4523–4533.

Li, J. (1993). Direction and polarization estimation using arrays with small loops and short dipoles. *IEEE Trans. Antennas Propagat.* **41**, 379–387.

Liu, X. and N. D. Sidiropoulos (2001). Camér-Rao lower bounds for low-rank decomposition of multidimensional arrays. *IEEE Trans. Signal Processing* **49**, 2074–2086.

Miron, S., N. Le Bihan and J. I. Mars (2005). Vector-sensor MUSIC for polarized seismic sources localisation. *EURASIP Journal on Applied Signal Processing* **2005**(1), 74–84.

Miron, S., N. Le Bihan and J. I. Mars (2006). Quaternion MUSIC for vector-sensor array processing. *IEEE Trans. Signal Process.* **54**(4), 1218–1229.

Nehorai, A. and E. Paldi (1994). Vector-sensor array processing for electromagnetic source localisation. *IEEE Trans. Signal Processing* **42**(2), 376–398.

Nehorai, A., K. C. Ho and B. T. G. Tan (1999). Minimum-noise-variance beamformer with an electromagnetic vector sensor. *IEEE Trans. Signal Processing* **47**(3), 601–618.

Nocedal, J. and S. J. Wright (2006). *Numerical Optimization*. Springer-Verlag. New York.

Rahamim, D., R. Shavit and J. Tabrikian (2003). Coherent source localisation using vector sensor arrays. *IEEE Int. Conf. Acoust., Speech, Signal Processing* pp. 141–144.

Rajih, M. and P. Comon (2005). Enhanced line search: A novel method to accelerate PARAFAC. In: *Proc. EUSIPCO 2005*. Antalya, Turkey.

Rife, D. C. and R. R. Boorstyn (1974). Single-tone parameter estimation from discrete-time observation. *IEEE Trans. Inform. Theory* **IT-20**(5), 591–598.

Rong, Y., S. A. Vorobyov, A. B. Gershman and N. D. Sidiropoulos (2005). Blind spatial signature estimation via time-varying user power loading and parallel factor analysis. *IEEE Trans. Signal Processing* **53**(5), 1697–1710.

Sidiropoulos, N. D. and R. Bro (2000). On the uniqueness of multilinear decomposition of N-way arrays. *Journal of chemometrics* (14), 229–239.

Sidiropoulos, N. D., G. B. Giannakis and R. Bro (2000*a*). Blind PARAFAC receivers for DS-CDMA systems. *IEEE Trans. Signal Processing* **48**(3), 810–823.

Sidiropoulos, N. D., R. Bro and G. B. Giannakis (2000*b*). Parallel factor analysis in sensor array processing. *IEEE Trans. Signal Processing* **48**(8), 2377–2388.

Swindlehurst, A., M. Goris and B. Ottersten (1997). Some experiments with array data collected in actual urban and suburban environments. In: *IEEE Workshop on Signal Proc. Adv. in Wireless Comm.*. Paris, France. pp. 301–304.

Tan, K.-C., K.-C. Ho and A. Nehorai (1996*a*). Linear independence of steering vectors of an electromagnetic vector sensor. *IEEE Trans. Signal Process.* **44**(12), 3099–3107.

Tan, K.-C., K.-C. Ho and A. Nehorai (1996*b*). Uniqueness study of measurements obtainable with arrays of electromagnetic vector sensors. *IEEE Trans. Signal Process.* **44**(4), 1036–1039.

Weiss, A. J. and B. Friedlander (1993*a*). Analysis of a signal estimation algorithm for diversely polarized arrays. *IEEE Trans. Signal Process.* **41**(8), 2628–2638.

Weiss, A. J and B. Friedlander (1993*b*). Direction finding for diversely polarized signals using polynomial rooting. *IEEE Trans. Signal Processing* **41**(5), 1893–1905.

Wong, K. T. and M. D. Zoltowski (1997). Uni-vector-sensor ESPRIT for multisource azimuth, elevation, and polarization estimation. *IEEE Trans. Antennas Propagat.* **45**(10), 1467–1474.

Zhang, X. and D. Xu (2007). Blind PARAFAC signal detection for polarization sensitive array. *EURASIP Journal on Advances in Signal Processing* **2007**, Article ID 12025, 7 pages.

Zoltowski, M. D. and K. T. Wong (2000*a*). Closed-form eigenstructure-based direction finding using arbitrary but identical subarrays on a sparse uniform cartesian array grid. *IEEE Trans. Signal Process.* **48**(8), 2205–2210.

Zoltowski, M. D. and K. T. Wong (2000*b*). ESPRIT-based 2-D direction finding with a sparse uniform array of electromagnetic vector sensors. *IEEE Trans. Signal Process.* **48**(8), 2195–2204.

Signal Processing
Edited by Sebastian Miron

ISBN 978-953-7619-91-6
Hard cover, 528 pages
Publisher InTech
Published online 01, March, 2010
Published in print edition March, 2010

This book intends to provide highlights of the current research in signal processing area and to offer a snapshot of the recent advances in this field. This work is mainly destined to researchers in the signal processing related areas but it is also accessible to anyone with a scientific background desiring to have an up-to-date overview of this domain. The twenty-five chapters present methodological advances and recent applications of signal processing algorithms in various domains as telecommunications, array processing, biology, cryptography, image and speech processing. The methodologies illustrated in this book, such as sparse signal recovery, are hot topics in the signal processing community at this moment. The editor would like to thank all the authors for their excellent contributions in different areas of signal processing and hopes that this book will be of valuable help to the readers.